Received: 27 September 2022 | Revised: 22 March 2023 | Accepted: 26 March 2023

DOI: 10.1111/mpp.13338

Molecular Plant Pathology WILEY

ORIGINAL ARTICLE

The neighbouring genes *AvrLm10A* and *AvrLm10B* are part of a large multigene family of cooperating effector genes conserved in Dothideomycetes and Sordariomycetes

Nacera Talbi[1] | Like Fokkens[2] | Corinne Audran[3] | Yohann Petit-Houdenot[1] | Cécile Pouzet[4] | Françoise Blaise[1] | Elise J. Gay[1] | Thierry Rouxel[1] | Marie-Hélène Balesdent[1] | Martijn Rep[2] | Isabelle Fudal[1]

[1]BIOGER, INRAE, Université Paris-Saclay, Palaiseau, France

[2]Molecular Plant Pathology, University of Amsterdam, Amsterdam, Netherlands

[3]UMR LIPME, Université de Toulouse, INRAE, CNRS, Castanet-Tolosan, France

[4]FRAIB-TRI Imaging Platform Facilities, FR AIB, Université de Toulouse, CNRS, Castanet-Tolosan, France

Correspondence
Isabelle Fudal, BIOGER, INRAE, Université Paris-Saclay, 22 place de l'Agronomie, 91120 Palaiseau, France.
Email: isabelle.fudal@inrae.fr

Present address
Like Fokkens, Laboratory of Phytopathology, Wageningen University and Research, Wageningen, Netherlands

Funding information
Agence Nationale de la Recherche, Grant/Award Number: ANR-10-LABX-41, ANR-14-CE19-0019 and ANR-17-EUR-0007; Institut National de Recherche pour l'Agriculture, l'Alimentation et l'Environnement; Université Paris-Saclay

Abstract

Fungal effectors (small-secreted proteins) have long been considered as species or even subpopulation-specific. The increasing availability of high-quality fungal genomes and annotations has allowed the identification of trans-species or trans-genera families of effectors. Two avirulence effectors, *AvrLm10A* and *AvrLm10B*, of *Leptosphaeria maculans*, the fungus causing stem canker of oilseed rape, are members of such a large family of effectors. *AvrLm10A* and *AvrLm10B* are neighbouring genes, organized in divergent transcriptional orientation. Sequence searches within the *L. maculans* genome showed that *AvrLm10A/AvrLm10B* belong to a multigene family comprising five pairs of genes with a similar tail-to-tail organization. The two genes, in a pair, always had the same expression pattern and two expression profiles were distinguished, associated with the biotrophic colonization of cotyledons and/or petioles and stems. Of the two protein pairs further investigated, AvrLm10A_like1/AvrLm10B_like1 and AvrLm10A_like2/AvrLm10B_like2, the second one had the ability to physically interact, similarly to what was previously described for the AvrLm10A/AvrLm10B pair, and cross-interactions were also detected for two pairs. AvrLm10A homologues were identified in more than 30 Dothideomycete and Sordariomycete plant-pathogenic fungi. One of them, SIX5, is an effector from *Fusarium oxysporum* f. sp. *lycopersici* physically interacting with the avirulence effector Avr2. We found that AvrLm10A/SIX5 homologues were associated with at least eight distinct putative effector families, suggesting that AvrLm10A/SIX5 is able to cooperate with different effectors. These results point to a general role of the AvrLm10A/SIX5 proteins as "cooperating proteins", able to interact with diverse families of effectors whose encoding gene is co-regulated with the neighbouring AvrLm10A homologue.

KEYWORDS
avirulence, *Brassica napus*, effector family, *Fusarium oxysporum*, *Leptosphaeria maculans*, pathogenic fungi, resistance

1 | INTRODUCTION

Host plant invasion by phytopathogenic fungi involves effectors, key elements of pathogenesis. They mainly correspond to secreted proteins that modulate plant immunity and facilitate infection (Lo Presti et al., 2015; Rocafort et al., 2020). Some effectors are recognized by resistance proteins (R) and are then termed avirulence (AVR) proteins. Recognition of a pathogen AVR protein triggers a set of immune responses grouped under the term effector-triggered immunity (ETI; Jones & Dangl, 2006). Pathogens typically escape recognition and overcome ETI by altering the effector protein, by ceasing expression of the effector gene, or by deleting the effector gene (Guttman et al., 2014; Jones & Dangl, 2006; Sánchez-Vallet et al., 2018). This evolutionary pressure leads to rapid diversification and turnover of effector genes. As a result, fungal effector proteins often have few recognizable homologues. This impairs reconstructions of effector evolution, for example whether new effectors have been acquired through horizontal transfer or duplication and divergence.

Leptosphaeria maculans 'brassicae' is an ascomycete of the Dothideomycete family that infects *Brassica* species, notably oilseed rape (*Brassica napus*), causing stem canker disease (also called blackleg). It has a long and complex hemibiotrophic lifecycle on its host, including two alternating biotrophic and necrotrophic phases on leaves and stems. The main strategy to control *L. maculans* 'brassicae' is genetic control combining specific *R* genes (called *Rlm*) and quantitative resistance (Brun et al., 2010; Delourme et al., 2004). During its lengthy interaction with the plant, *L. maculans* 'brassicae' expresses putative effector genes in eight waves, often specific to a lifestyle (biotrophy, transition from biotrophy to necrotrophy, necrotrophy) or tissue (Gay et al., 2021). One of these waves includes effector genes expressed during the asymptomatic stages of leaf, petiole, and stem colonization (biotrophy effectors), among which are the 12 *AVR* genes that have been identified so far in *L. maculans* 'brassicae', referred to as *AvrLm* genes (Balesdent et al., 2013; Degrave et al., 2021; Fudal et al., 2007; Ghanbarnia et al., 2015, 2018; Gout et al., 2006; Jiquel et al., 2021; Neik et al., 2022; Parlange et al., 2009; Petit-Houdenot et al., 2019; Plissonneau et al., 2016; Van de Wouw et al., 2014).

The genome of *L. maculans* 'brassicae' has a well-defined bipartite structure composed of gene-rich, GC-equilibrated regions and of gene-poor, AT-rich regions enriched in transposable elements (TEs) that are truncated and degenerated by repeat-induced point mutation (RIP) (Dutreux et al., 2018; Rouxel et al., 2011). Effector genes in AT-rich regions have been shown to experience deletions and single-nucleotide polymorphisms (SNPs), and can accumulate mutations induced by RIP that enable *L. maculans* 'brassicae' to escape host resistance gene recognition (Daverdin et al., 2012; Fudal et al., 2009; Grandaubert et al., 2014). Biotrophy effectors, including the 12 *AvrLm* genes, are typically associated with AT-rich regions.

Several AVR proteins of *L. maculans* 'brassicae' were found to display limited sequence identity with those of other plant-pathogenic fungi: homologues of AvrLm6 were identified in two *Venturia* species, *V. inaequalis* and *V. pirina* (Shiller et al., 2015), AvrLm3 was shown to have sequence homology with Ecp11-1, an AVR protein of *Fulvia fulva* (Mesarich et al., 2018), and a structural family including AvrLm4-7, AvrLm5-9, AvrLm3, and AvrLmS-Lep2 was identified in *L. maculans* 'brassicae' and other plant-pathogenic fungi (Lazar et al., 2022). The most striking example of conserved *AVR* genes is the case of *AvrLm10A* and *AvrLm10B*, two neighbouring genes localized in an AT-rich subtelomeric region, organized in divergent transcriptional orientation (Petit-Houdenot et al., 2019). They are co-expressed and their encoded proteins were found to physically interact. *AvrLm10A* and *AvrLm10B* are both necessary to trigger Rlm10-mediated resistance: silencing of only one of the two genes is sufficient to escape Rlm10-mediated recognition, while complementation with the two genes and their intergenic region is necessary to trigger recognition. Together, these findings strongly indicate that these effectors closely cooperate during infection. Preliminary analyses suggested that *AvrLm10A* and *AvrLm10B* (and their genome organization) were conserved in several Dothideomycetes and Sordariomycetes species (Petit-Houdenot et al., 2019). Compared to AvrLm10B, AvrLm10A has a higher number of orthologues (10 instead of seven), including SIX5, an effector previously described in *Fusarium oxysporum* f. sp. *lycopersici*. *SIX5* is organized in a gene pair with another effector, *AVR2*, that is not homologous to *AvrLm10B*. Like AvrLm10A and AvrLm10B, SIX5 and Avr2 physically interact and cooperate during infection (Cao et al., 2018; Ma et al., 2015), indicating that functional relations can be conserved over longer evolutionary distances and with different proteins. Very few examples of effector cooperation have been reported in fungi. Recently, in *F. oxysporum* f. sp. *conglutinans*, the effector PSE was also found to have an effector partner, SIX8, encoded by a neighbouring gene in inverse orientation. The two effectors are able to physically interact and to suppress phytoalexin production and plant immunity in *Arabidopsis thaliana* (Ayukawa et al., 2021).

Here we investigated the functional and evolutionary conservation of the AvrLm10 module. We searched for homologous protein pairs of AvrLm10A/AvrLm10B in *L. maculans* 'brassicae' and identified four pairs of paralogues. We first studied the conservation of these pairs in different *L. maculans* 'brassicae' populations and compared their expression dynamics during oilseed rape infection. Then, we tested the ability of some of the corresponding proteins to interact physically. Finally, we studied conservation of AvrLm10A/AvrLm10B over longer evolutionary distances and found that AvrLm10A is conserved in more than 30 Dothideomycetes and Sordariomycetes, but identified only 11 homologues for AvrLm10B. Interestingly, multiple distant homologues of AvrLm10A are, like SIX5 and Avr2, paired with a neighbouring gene that is not homologous to AvrLm10B, suggesting multiple cases of nonorthologous replacement of the AvrLm10B component of this module. These results point to a general role of the AvrLm10A proteins as cooperating proteins, able to physically interact with diverse families

of effectors and to potentially share a conserved function during plant infection.

2 | RESULTS

2.1 | Several *AvrLm10A/AvrLm10B* homologues are present in the *L. maculans* 'brassicae' genome as gene pairs

We used BlastP to search for homologues of AvrLm10A/AvrLm10B in the proteome of *L. maculans* 'brassicae' JN3 (v23.1.3). We identified four homologues for AvrLm10A (Lmb_jn3_07875): Lmb_jn3_08094 (AvrLm10A_like1), Lmb_jn3_09745 (AvrLm10A_like2), Lmb_jn3_04095 (AvrLm10A_like3), and Lmb_jn3_02612 (AvrLm10A_like4). Amino acid sequences of these homologues range in size from 120 to 124 amino acids, are 36% to 51% identical to AvrLm10A, and have a conserved number of cysteines (seven cysteines in the mature protein; Tables 1 and 2). The corresponding genes, like *AvrLm10A*, all have three introns, located at the same relative positions. For AvrLm10B (Lmb_jn3_07874) we also identified four homologues: Lmb_jn3_08095 (AvrLm10B_like1), Lmb_jn3_09746 (AvrLm10B_like2), Lmb_jn3_04096 (AvrLm10B_like3), and Lema_P017580.1 (AvrLm10B_like4). This latter gene was predicted in the first version of the *L. maculans* genome annotation but is absent from the latest annotation due to lack of transcriptomic support (Dutreux et al., 2018; Rouxel et al., 2011). These homologues range in size between 166 and 180 amino acids, share between 25% and 34% identity, and contain only one cysteine (except for AvrLm10B_like2, which contains two; Tables 1 and 2). The corresponding genes share one intron either located at the end of the coding sequence or in the 3′ untranslated region (UTR). For all proteins that belong to the AvrLm10A or AvrLm10B families, a secretion signal peptide was predicted.

Interestingly, like *AvrLm10A* and *AvrLm10B*, all these homologues were organized as neighbouring gene pairs in diverging orientation. While *AvrLm10A* and *AvrLm10B* are separated by a large (7213 bp) repeat-rich intergenic region, the other gene pairs are separated by smaller intergenic regions, ranging between 692 bp and 1.2 kb (Table 1). All gene pairs are located on different scaffolds. *AvrLm10A_like2* and *AvrLm10B_like2*, as *AvrLm10A* and *AvrLm10B*, are located in an AT-rich, repeat-rich, and gene-poor subtelomeric region. *AvrLm10A_like3/AvrLm10B_like3* is also located in a subtelomeric AT-rich region, but adjacent to a gene-rich region. The *AvrLm10A_like1/AvrLm10B_like1* gene pair is located in a gene cluster of seven genes on an AT-isochore that is not subtelomeric. Finally, the *AvrLm10A_like4/AvrLm10B_like4* gene pair is located in a GC-isochore (Table 1).

In summary, the four homologues of AvrLm10A and AvrLm10B share similar characteristics in their amino acid sequence (size, cysteine number, prediction of a signal peptide) and the corresponding genes share the same organization (genes pairs in diverging orientation, same number of introns) but are found in different genomic environments.

2.2 | Most members of the *AvrLm10* family are highly conserved in *L. maculans* field populations

To compare the conservation of *AvrLm10A*, *AvrLm10B*, and their homologues in different *L. maculans* populations, we determined their presence by PCR on a worldwide collection of 150 *L. maculans* isolates (Tables S1 and S2). We included isolates from most of the rapeseed-producing regions where *L. maculans* is present (Table S2). In general, presence/absence polymorphisms are identical for the two genes forming a pair (Figure 1 and Table S3). Excluding the *AvrLm10A_like2/AvrLm10B_like2* pair that was absent in most isolates from Mexico (absent in 94% of isolates) and Australia (absent in 59% of isolates), the four other pairs were present in the vast majority of isolates (between 92% and 99%).

We also analysed sequence polymorphism in a subset of isolates (Tables 3 and S3). Sequence polymorphisms were rare for most pairs: only one mutation was detected in an intron of *AvrLm10A_like1* in a single isolate, and a single nonsynonymous point mutation in *AvrLm10B_like3* for an Australian isolate, leading to a $D^{178}N$ change (Table 3). *AvrLm10A* and *AvrLm10B* displayed two SNPs in 46.5% and 50%, respectively, of the analysed isolates, with only one SNP leading to an amino acid change in AvrLm10B ($M^{92}I$). In contrast, *AvrLm10A_like2* and *AvrLm10B_like2* displayed high sequence variation with four alleles, including 13 polymorphic sites, and five alleles, including 17 polymorphic sites, respectively. These polymorphisms were detected in only 15.6% of the isolates due to numerous presence/absence polymorphisms (Table 3). Importantly, most SNPs were located in exons and resulted in amino acid changes. In an Australian isolate (WT75), both genes displayed many G to A and C to T mutations, suggesting that RIP contributed to mutation accumulation in this isolate. We calculated RIP indexes as defined by Galagan et al. (2003) and indeed observed an increase of the TpA/ApT index for the alleles of *AvrLm10A_like2* and *AvrLm10B_like2* present in WT75.

In conclusion, members of the *AvrLm10* family are highly conserved in *L. maculans* field populations, with the exception of *AvrLm10A_like2/AvrLm10B_like2*, which are frequently absent together and show sequence polymorphism.

2.3 | Gene pairs within the *AvrLm10* family are co-expressed during oilseed rape infection by *L. maculans* in two distinct expression clusters

To determine to what extent the two components of a pair function together, we studied their expression profiles using RNA-seq data previously generated by Gay et al. (2021). These data included cotyledon, petiole, and stem colonization by *L. maculans* under controlled conditions (Figure 2a). No expression of *AvrLm10A_like4* and *AvrLm10B_like4* could be detected in any of the conditions tested, including infection in controlled conditions, field infection, residues, and axenic growth (data not shown). In contrast, expression was detected for all the other genes, and within each pair both components

TABLE 1 Characteristics of AvrLm10A and AvrLm10B homologous proteins identified in *Leptosphaeria maculans* 'brassicae'

Protein	Coordinates on the genome	Size (aa)	Cysteine number[a]	Identity with AvrLm10A	Protein	Coordinates on the genome	Size (aa)	Cysteine number[a]	Identity with AvrLm10B	Localization in the genome[b]	Size of the intergenic region (bp)
AvrLm10A	JN3_SC08: 2235860–2236381	120	7	—	AvrLm10B	JN3_SC08: 2228122–2228647	178	1	—	AT-isochore (subtelomeric region; end of SC8)	7600
AvrLm10A-like1 (Lmb_jn3_08094)	JN3_SC09: 793880–794422	123	7	40%	AvrLm10B-like1 (Lmb_jn3_08095)	JN3_SC09: 795122–795624	171	1	27%	GC-isochore (SC09, island of 7 genes in AT-isochore)	699
AvrLm10A-like2 (Lmb_jn3_09745)	JN3_SC11: 1893710–1894257	120	7	36%	AvrLm10B-like2 (Lmb_jn3_09746)	JN3_SC11: 1894950–1895450	166	2	25%	AT-isochore (subtelomeric region; end of SC11)	692
AvrLm10A-like3 (Lmb_jn3_04095)	JN3_SC04: 85542–86091	124	7	36%	AvrLm10B-like3 (Lmb_jn3_04096)	JN3_SC04: 87305–87900	180	1	32%	GC-isochore border (subtelomeric region; end of SC4)	1200
AvrLm10A-like4 (Lmb_jn3_02612)	JN3_SC02: 1621177–1621720	123	7	51%	AvrLm10B-like4 (Lema_P017580.1)	JN3_SC02: 1619918–1620457	179	1	34%	GC-isochore (SC02)	719

[a]Cysteine number is calculated based on the mature protein, without signal peptide.

[b]SC: Supercontig (based on the Dutreux et al. (2018) *L. maculans* genome assembly).

TABLE 2 Percentage of identity between members of the AvrLm10 family in *Leptosphaeria maculans* 'brassicae'

	AvrLm10A-like1	AvrLm10A-like2	AvrLm10A-like3	AvrLm10A-like4
AvrLm10A	40% (56.0%)	36% (54%)	36% (50%)	51% (64%)
AvrLm10A-like1		50% (62%)	54% (65%)	40% (55%)
AvrLm10A-like2			54% (67%)	37% (50%)
AvrLm10A-like3				38% (49%)
	AvrLm10B-like1	**AvrLm10B-like2**	**AvrLm10B-like3**	**AvrLm10B-like4**
AvrLm10B	27% (38%)	25% (41%)	32% (39%)	34% (47%)
AvrLm10B-like1		32% (45%)	35% (47%)	28% (50%)
AvrLm10B-like2			34% (44%)	28% (43%)
AvrLm10B-like3				24% (38%)

Note: The identity (similarity) matrix was obtained by performing a reciprocal BlastP using the BioEdit sequence alignment editor (matrix: BLOSUM62, E-value = 1).

were clearly co-expressed (Figure 2a). All the genes were overexpressed during infection at biotrophic stages of colonization on cotyledons, and/or petioles and stems compared to axenic growth on V8 medium. However, two patterns could be distinguished: *AvrLm10A_like2/AvrLm10B_like2* and *AvrLm10A/AvrLm10B* both showed a typical expression profile of the biotrophy effectors with overexpression at all the stages of biotrophic colonization, while *AvrLm10A_like1/AvrLm10B_like1* and *AvrLm10A_like3/AvrLm10B_like3* were only overexpressed during biotrophic colonization of petioles and stems.

The expression of the *AvrLm10* family was then validated by reverse transcription-quantitative PCR (RT-qPCR) (Figure 2b). This confirmed co-expression of the gene pairs *AvrLm10A/AvrLm10B*, *AvrLm10A_like1/AvrLm10B_like1*, and *AvrLm10A_like2/AvrLm10B_like2*, consistent with the expression patterns observed using RNA-seq data. In contrast, the RT-qPCR experiments suggested that *AvrLm10B_like3* was expressed 10 times less than *AvrLm10A_like3*.

2.4 | AvrLm10A_like1, AvrLm10B_like1, AvrLm10A_like2, and AvrLm10B_like2 colocalize in the nucleus and cytoplasm of *Nicotiana benthamiana* cells when transiently expressed

It was previously shown that both AvrLm10A and AvrLm10B exhibited nucleocytoplasmic localization when transiently expressed in leaves of *N. benthamiana* (Petit-Houdenot et al., 2019). We tested whether the same holds true for the pairs that were shown to be co-expressed. AvrLm10A_like1/AvrLm10A_like2 and AvrLm10B_like1/AvrLm10B_like2 fused to green fluorescent protein (GFP) and red fluorescent protein (RFP), respectively, at the C- or N-terminal position, were transiently expressed in leaf epidermal cells of *N. benthamiana* without their secretion signal peptide. When AvrLm10A_like1/AvrLm10B_like1 or AvrLm10A_like2/AvrLm10B_like2 proteins were co-expressed in *N. benthamiana*, they colocalized in the cytoplasm and nucleus (Figure 3a). Immunoblot analysis with anti-GFP and anti-RFP antibodies confirmed the presence of the intact recombinant proteins (Figures 3b and S1).

2.5 | AvrLm10A_like2 physically interacts with AvrLm10B_like2 in planta

Having established that AvrLm10A_like1/AvrLm10B_like1 and AvrLm10A_like2/AvrLm10B_like2, like AvrLm10A/AvrLm10B, colocalize in the nucleus and cytoplasm of *N. benthamiana* cells, we examined whether these pairs physically interact in planta. Co-immunoprecipitation (CoIP) experiments were performed to test physical interactions in planta. Immunoblotting using anti-RFP antibody indicated that all constructs were highly expressed (Figure 3b). Immunoprecipitation of proteins using anti-RFP beads revealed, after immunoblotting with anti-GFP antibodies, that AvrLm10A_like2 was coprecipitated with AvrLm10B_like2, but not with RFP. In contrast, AvrLm10A_like1 did not coprecipitate with either AvrLm10B_like1 or RFP.

An in planta-fluorescence resonance energy transfer–fluorescence lifetime imaging microscopy (FRET-FLIM) analysis was also performed. AvrLm10A_like1/AvrLm10A_like2 and AvrLm10B_like1/AvrLm10B_like2, fused to GFP and RFP, respectively, were expressed in leaf epidermal cells of *N. benthamiana*. FRET-FLIM experiments were performed on the cytoplasm of cotransformed cells. LmStee98 fused to RFP that was previously detected in the cytoplasm and the nucleus of *N. benthamiana* cells (Jiquel, 2021) was used as a negative control. The lifetime of GFP fluorescence was highly reduced in cells co-expressing AvrLm10A_like2-GFP and AvrLm10B_like2-RFP compared with cells expressing AvrLm10A_like2-GFP alone or co-expressing AvrLm10A_like2-GFP and LmStee98-RFP (Table 4). This is indicative of interaction between AvrLm10A_like2 and AvrLm10B_like2 in planta. In contrast, co-expression of AvrLm10A_like1-GFP and AvrLm10B_like1-RFP (or RFP-AvrLm10B_like1) did not result in significant reduction of the GFP fluorescence lifetime despite the same subcellular colocalization of both proteins (Table 4). Taken together, these results suggest that AvrLm10A_like2

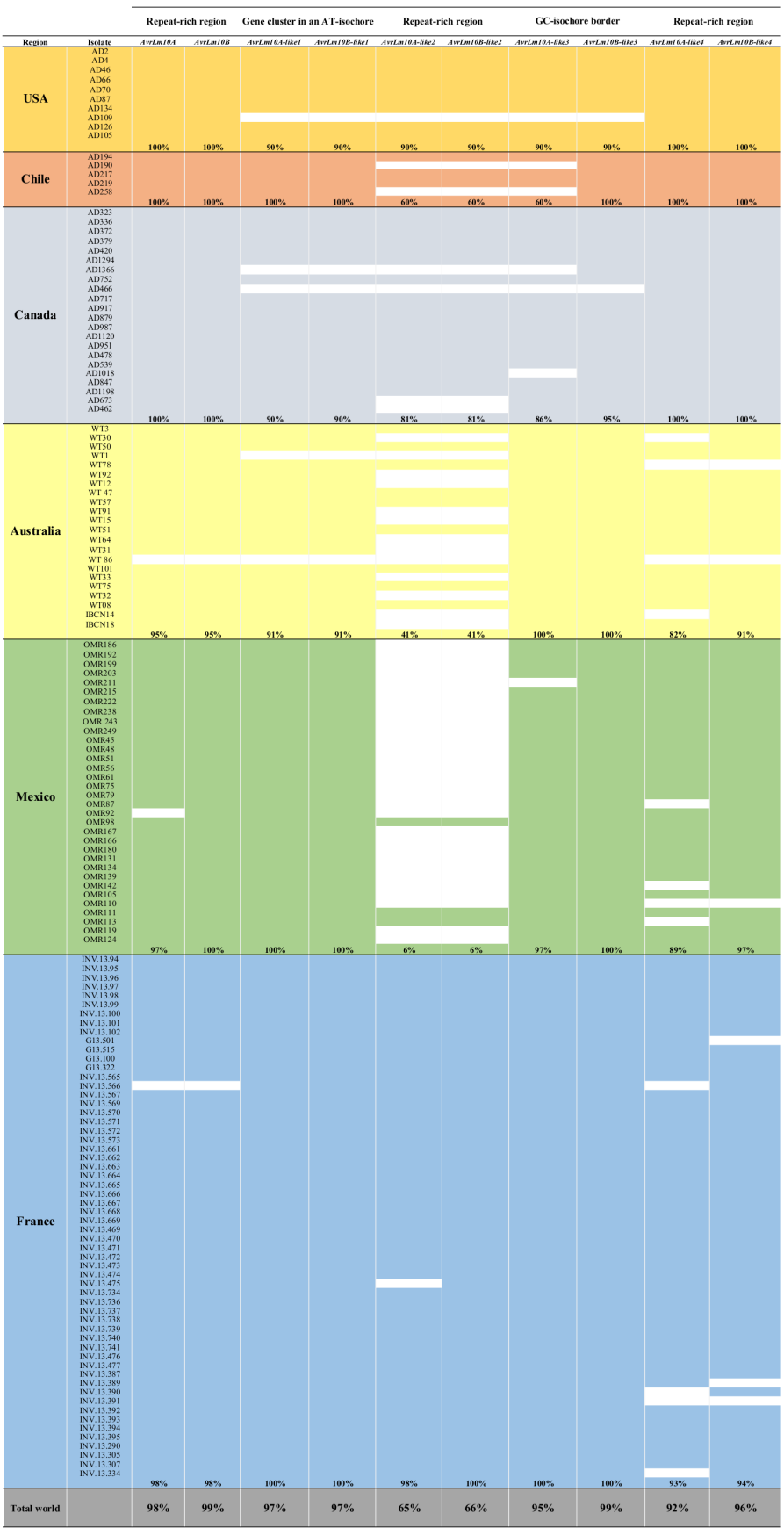

FIGURE 1 Presence of the *AvrLm10* family in natural populations of *Leptosphaeria maculans* 'brassicae'. Presence of the genes was evaluated by PCR using 5′ and 3′ untranslated region (UTR)-specific primers (see Table S1). Absence of a gene amplification is represented by a white box.

TABLE 3 Allelic variants identified within the *AvrLm10* family in natural isolates of *Leptosphaeria maculans* and influence of repeat-induced point mutation on sequence variation

Allele	G+C content (%)	Nucleotide change	Localization (intron/exon)	Amino acid change	Number of isolates (%)	CpA occurrence[a] (O/E)	TpG occurrence[a] (O/E)	TpA occurrence[a] (O/E)	TpA/ApT[b]	CpA+TpG / ApC+GpT[b]
AvrLm10-A_0	45.98	–	–	–	21/30 (53.5)	–	–	–	0.91	1.33
AvrLm10-A_1	45.59	$G^{41}A$	Intron 1	No	18/39 (46.5)	1	0.97	0.97	0.94	1.34
		$C^{327}A$	Intron 3	No						
AvrLm10-B_0	47.43	–	–	–	17/34 (50.0)	–	–	–	0.8	1.23
AvrLm10-B_1	47.43	$A^{273}G$	Exon	No	17/34 (50.0)	1	0.97	0.97	0.8	1.23
		$G^{276}A$	Exon	$M^{92}I$						
AvrLm10A-like1_0	44.65	–	–	–	45/46 (97.8)	–	–	–	1.10	1.27
AvrLm10A-like1_1	44.55	$C^{69}T$	Intron 1	No	1/46 (2.2)	1	1	0.98	1.05	1.29
AvrLm10B-like1_0	44.65	–	–	–	47/47 (100)	–	–	–	1.10	1.27
AvrLm10A-like2_0	39.23	–	–	–	37/44 (84.1)	–	–	–	1.24	1.24
AvrLm10A-like2_1	39.42	$T^{202}C$	Exon 2	No	2/44 (4.5)	1	0.97	1	1.24	1.23
AvrLm10A-like2_2	39.05	$T^{55}A$	Intron 1	No	1/44 (2.3)	1	1.03	0.98	1.22	1.26
		$G^{159}T$	Exon 2	$R^{27}M$						
AvrLm10A-like2_3	37.59	$C^{73}T$	Intron 1	No	1/44 (2.3)	0.85	0.97	1.12	1.37	1.15
		$C^{82}T$	Intron 1	No						
		$G^{115}A$	Intron 1	No						
		$C^{138}T$	Exon 2	Q^{21}Stop						
		$C^{291}T$	Exon 3	$Q^{53}L$						
		$C^{298}T$	Exon 3	S^{54}Stop						
		$G^{313}A$	Exon 3	W^{59}Stop						
		$C^{454}T$	Exon 4	$S^{89}L$						
		$C^{549}T$	Exon 4	$S^{120}L$						
AvrLm10A-like2_4	39.23	$C^{346}G$	Exon 3	No	3/44 (6.8)	0.97	1	1	1.24	1.23
AvrLm10B-like2_0	46.51	–	–	–	29/45 (64.4)	–	–	–	0.67	1.39
AvrLm10B-like2_1	46.51	$T^{478}A$	Exon	$S^{160}T$	6/45 (13.3)	1	1	1.03	0.7	1.37
AvrLm10B-like2_2	46.51	$G^{328}A$	Exon	$G^{110}S$	1/45 (2.2)	1	0.96	1	0.67	1.42
		$T^{478}G$	Exon	$S^{160}A$						

TABLE 3 (Continued)

Allele	G+C content (%)	Nucleotide change	Localization (intron/exon)	Amino acid change	Number of isolates (%)	CpA occurrence[a] (O/E)	TpG occurrence[a] (O/E)	TpA occurrence[a] (O/E)	TpA/ApT[b]	CpA+TpG / ApC+GpT[b]
AvrLm10B-like2_3	44.51	$G^{86}A$	Exon	$R^{29}Q$	1/45 (2.2)	1.05	0.69	1.28	0.84	1.3
		$G^{157}A$	Exon	No						
		$G^{168}A$	Exon	$M^{56}I$						
		$G^{232}A$	Exon	$G^{78}R$						
		$G^{274}A$	Exon	$E^{92}K$						
		$G^{280}A$	Exon	No						
		$G^{318}A$	Exon	$M^{106}I$						
		$G^{379}A$	Exon	$E^{127}K$						
		$G^{451}A$	Exon	No						
		$G^{488}A$	Exon	W^{163}Stop						
AvrLm10B-like2_4	46.51	$T^{478}G$	Exon	$S^{160}A$	7/45 (15.6)	1	1.04	1	0.67	1.39
		$G^{484}T$	Exon	$A^{162}S$						
AvrLm10B-like2_5	46.71	$G^{347}C$	Exon	No	1/45 (2.2)	1.02	1.04	1	0.67	1.44
		$T^{478}G$	Exon	$S^{160}A$						
AvrLm10A-like3_0	45.64	–	–	–	35/35 (100)	–	–	–	1.46	1.21
AvrLm10B-like3_0	43.62	–	–	–	39/40 (97.5)	–	–	–	1	1.14
AvrLm10B-like3_1	43.79	$A^{533}C$	Exon	$D^{178}A$	1/40 (2.5)	1	31	1	1.02	1.14
AvrLm10A-like4_0	48.00	–	–	–	44/44 (100)	–	–	–	0.88	1,37
AvrLm10B-like4_0	49.90	–	–	–	44/44 (100)	–	–	–	0.62	1.40

[a]Dinucleotide frequencies: expressed as the observed occurrence over the expected number (O/E).

[b]TpA/ApT >2.0 or CpA + TpG/ApC + GpT <0.7 corresponds to regions predicted as repeat-induced point-mutated in *Neurospora crassa*, according to Galagan et al. (2003).

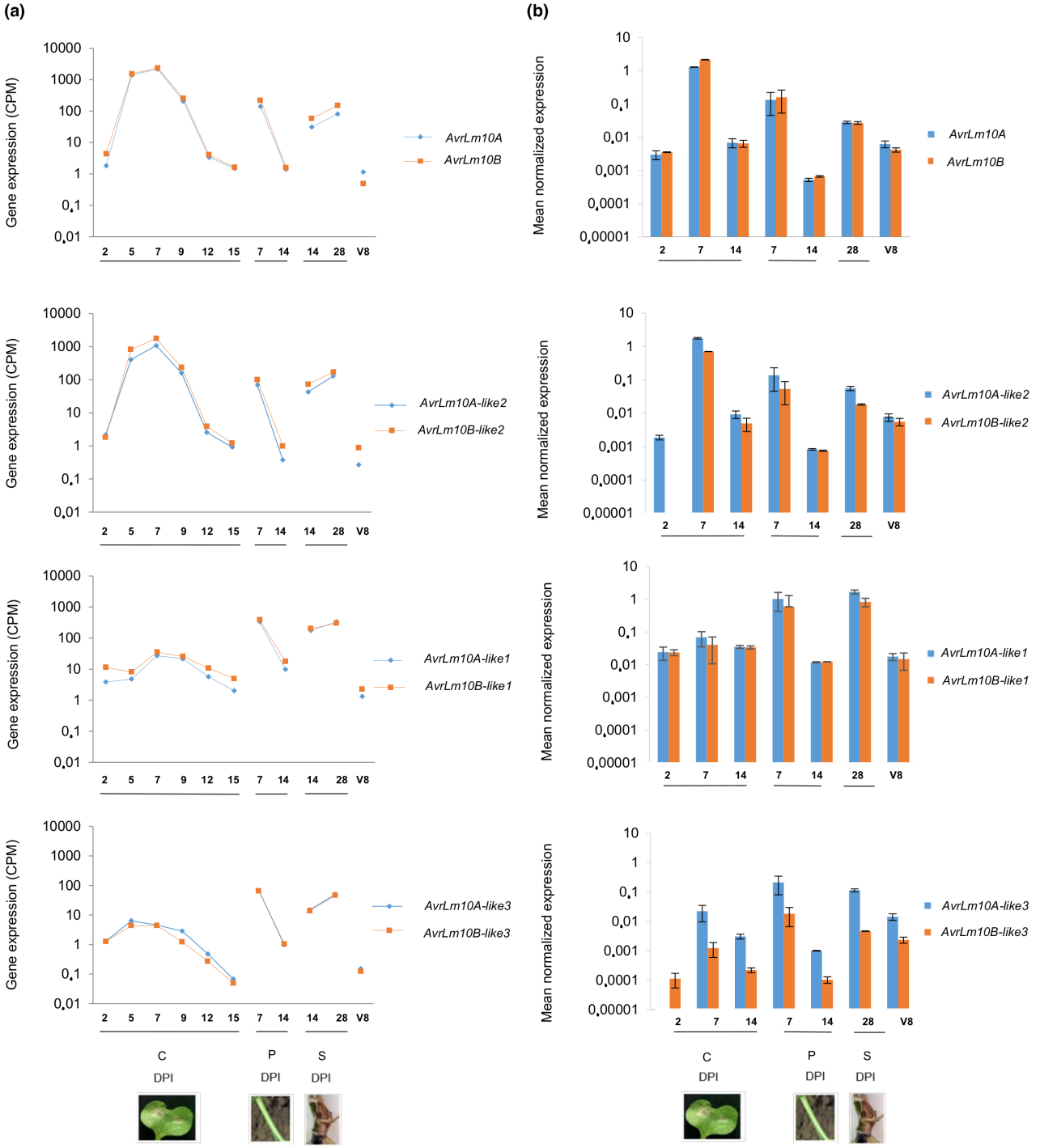

FIGURE 2 Expression of the *AvrLm10* family during oilseed rape infection by *Leptosphaeria maculans* 'brassicae'. (a) Expression pattern of the *AvrLm10* gene family using RNA-seq data generated by Gay et al. (2021) and normalized by the total number of sequences per condition (count per million, CPM). Each data point is the average of two independent biological replicates. (b) Expression pattern of the *AvrLm10* gene family analysed by reverse transcription-quantitative PCR. Gene expression levels are relative to *EF1α*, a constitutively expressed gene, according to Muller et al. (2002). Each data point is the average of two biological replicates and two technical replicates. Standard error of the mean normalized expression level is indicated by error bars. RNA extractions were performed on cotyledons, petioles, and stems of oilseed rape (Darmor-*bzh*) inoculated under controlled conditions with the reference isolate v23.1.2 and recovered at different dates (days postinoculation, DPI) on cotyledons (C), petioles (P), and stems (S).

and AvrLm10B_like2 physically interact in planta, while AvrLm10A_like1 and AvrLm10B_like1 do not.

Finally, using the same FRET-FLIM strategy, we tested cross-interactions between AvrLm10A/AvrLm10B and AvrLm10A_like2/AvrLm10B_like2, the two pairs sharing the same expression kinetics during oilseed rape infection (Table S4). These experiments suggested that AvrLm10A could interact with AvrLm10B_like2 and AvrLm10A_like2 with AvrLm10B in planta.

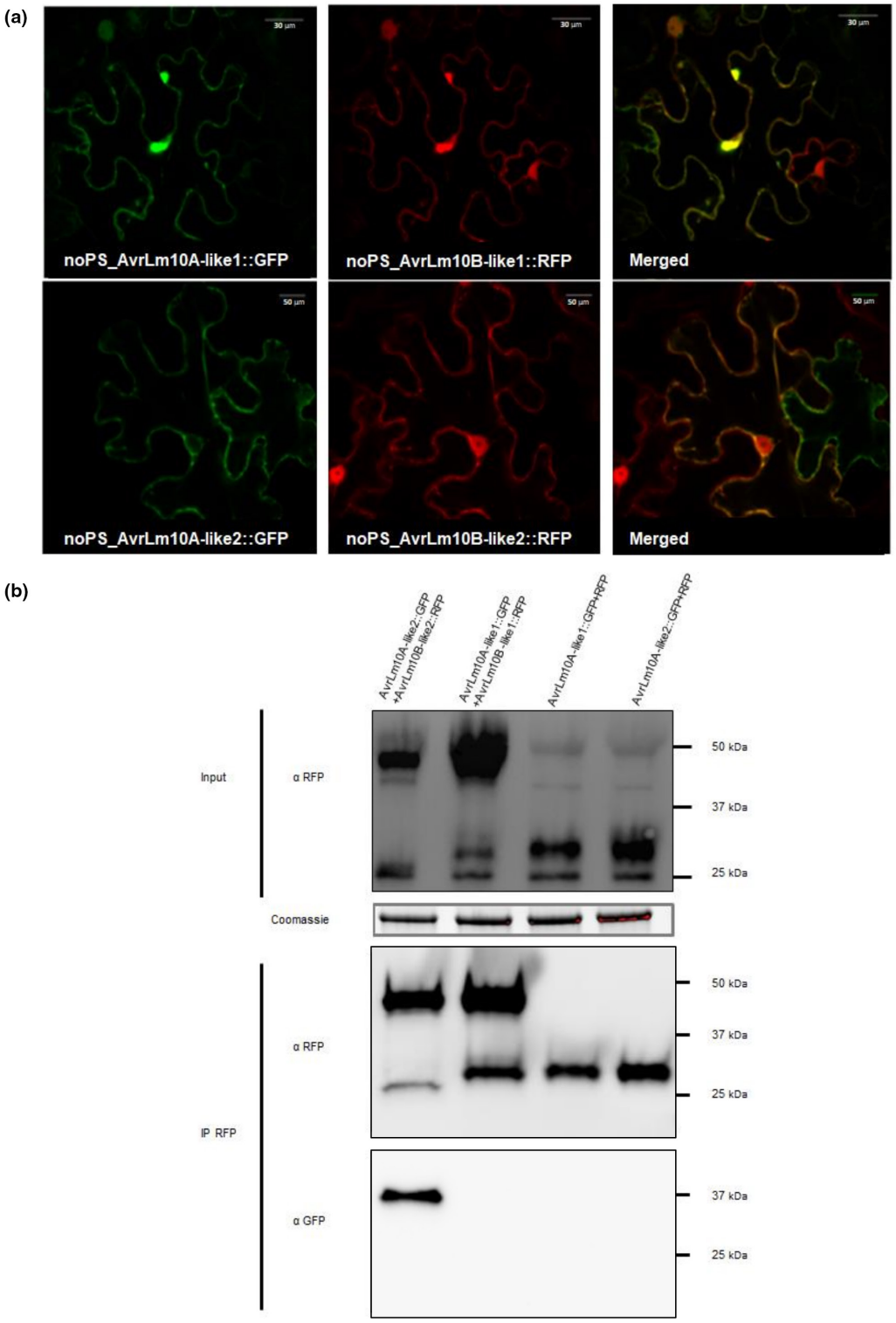

FIGURE 3 AvrLm10A_like1, AvrLm10B_like1, AvrLm10A_like2, and AvrLm10B_like2 co-localize in *Nicotiana benthamiana* cells, but only AvrLm10A_like2 and AvrLm10B_like2 physically interact. (a) Single-plane confocal images of *N. benthamiana* epidermal leaf cells expressing AvrLm10A_like1-GFP, AvrLm10B_like1-RFP, AvrLm10A_like2-GFP, and AvrLm10B_like2-RFP at 48 h postinfiltration of *Agrobacterium tumefaciens*. (b) Proteins were extracted 48 h after infiltration and analysed by immunoblotting with anti-RFP (α-RFP) antibodies (Input). Immunoprecipitation was performed with anti-RFP beads (IP RFP) and analysed by immunoblotting with anti-RFP antibodies to detect AvrLm10B_like1-RFP, AvrLm10B_like2-RFP, and RFP, and with anti-GFP (α-GFP) antibodies for the detection of co-immunoprecipitated proteins.

TABLE 4 FRET-FLIM analysis showing a strong physical interaction between AvrLm10A-like2 and AvrLm10B-like2

Donor	Acceptor	τ[a]	*SEM*[b]	Δt[c]	*n*[d]	*E*[e]	*p* value[f]
AvrLm10A-like1-GFP	–	2.96	0.009	–	88	–	–
AvrLm10A-like1-GFP	RFP-AvrLm10B-like1	2.87	0.012	0.09	78	3.145	1.52×10^{-9}
AvrLm10A-like1-GFP	AvrLm10B-like1-RFP	2.90	0.012	0.07	72	2.253	7.93×10^{-6}
AvrLm10A-like2-GFP	–	2.79	0.011	–	100	–	–
AvrLm10A-like2-GFP	AvrLm10B-like2-RFP	1.89	0.029	0.90	90	32.126	4.37×10^{-73}
AvrLm10A-like2-GFP	LmStee98-RFP	2.77	0.016	0.02	66	0.721	0.282

[a]Mean lifetime in nanoseconds, calculated according to $\tau=\Sigma\alpha_i\tau_i^2/\Sigma\alpha_i\tau_i$ with $I(t)=\Sigma\alpha_i e^{-t/\pi}$.

[b]Standard error of the mean.

[c]$\Delta t=\tau D-\tau DA$, expressed in nanoseconds, where τD is the lifetime in the absence of the acceptor and τDA is the lifetime of the donor in the presence of the acceptor.

[d]Total number of measured cells.

[e]Percentage of FRET efficiency ($E=1-\tau DA/\tau D$).

[f]*p* value of the difference between the donor lifetimes in the presence and in the absence of the acceptor (Student's *t* test).

2.6 | The AvrLm10A/Six5 family is conserved in several phytopathogenic fungi and can be divided into three clades with specific cysteine patterns

We wondered to what extend the AvrLm10 module is conserved in other species. Previous analyses have shown that AvrLm10A is homologous to SIX5, an effector protein in *F. oxysporum* f. sp. *lycopersici;* therefore, we used AvrLm10A and its four homologues in *L. maculans* 'brassicae' and SIX5 as a query in BlastP searches. We identified a total of 65 additional homologues, most of which are in *Colletotrichum* or *Fusarium* species, bringing the total size of the AvrLm10A/SIX5 family members to 71. We exclusively found homologues in Dothideomycete, Sordariomycete, and Leotiomycete phytopathogenic fungi (Table S5), with one exception: *Penicillium polonicum*, a Eurotiomycete that is not phytopathogenic but known to spoil stored plant products. Some species carry several members of the AvrLm10A family with a maximum of three homologues within a genome (Figure S2).

We generated a multiple sequence alignment for the 71 members of the AvrLm10A/SIX5 family. Although the protein sequences have diverged a lot, we could identify a few residues that were conserved in all members. These include CACQ, a cysteine at alignment position 157 and DSTCF near the C-terminus. We then used this alignment to infer a phylogenetic tree (Figure 4). Based on the alignment and the tree, we distinguished three clades, each with a distinct pattern of cysteines. The first clade consists of 25 proteins, mostly from Sordariomycetes, but also Dothideomycetes and the Eurotiomycete *P. polonicum*. Proteins in this clade are characterized by relatively short protein sequences (97 amino acids on average) that typically have two cysteines at alignment positions 85 and 96, one at alignment position 131, and two at alignment positions 156 and 157 (Figure 5a). A major part of this clade consists of tandemly duplicated genes in *F. oxysporum* (T in Figure 4). The second clade consists of 10 proteins, all from Dothideomycetes, with an average size of 119 amino acids. These proteins have no clade-specific conserved cysteines but do have 11–28 amino acids extra between the signal peptide and the conserved CACQ motif (Figure 5b). Finally, the third clade consists of 36 proteins including the sequences of AvrLm10A, all its homologues in *Leptosphaeria* species, and SIX5. The clade contains proteins from Sordariomycetes, Dothideomycetes, and the Leotiomycete *Rhynchosporium agropyri*. Proteins in this group are on average 125 amino acids long and characterized by cysteines on alignment positions 90, 157 and 190 and a tryptophan on alignment position 112 (Figure 5c).

We conservatively annotated the gene tree and designated all internal nodes for which we find the same strain in both descending branches as duplications (red stars in Figure 4). We found a few recent expansions, for example within the second clade in Dothideomycetes, and species-specific duplications in *Venturia nashicola* and *L. maculans* 'brassicae'. Most duplications, however, seem to have occurred before the split of Dothideomycetes and Sordariomycetes or even before. These expansions have been succeeded by losses of one or both copies in most lineages, resulting in a patchy presence/absence pattern of subfamilies in different species.

2.7 | Eight different families of putative effector genes are associated with AvrLm10A/SIX5 subclades

To explore the presence of AvrLm10B and its homologues in other species, we used BlastP with AvrLm10B and its four *L. maculans* 'brassicae' homologues as queries. We identified 11 proteins in plant-pathogenic fungal species belonging to the Dothideomycetes and Sordariomycetes (only in *Colletotrichum* sp.; Table S6). Interestingly, all homologues of AvrLm10B were encoded by genes adjacent to a gene encoding a homologue of AvrLm10A, in the opposite orientation. Moreover, all the AvrLm10A homologues associated with an AvrLm10B homologue belong to the same subclade of clade III (Figure 4, black squares) and all members of this clade are thus associated with an AvrLm10B homologue.

The fact that the AvrLm10A/SIX5 family is present in more species than the AvrLm10B family (32 instead of 25) suggests that members of the AvrLm10A/SIX5 may function on their own or together with

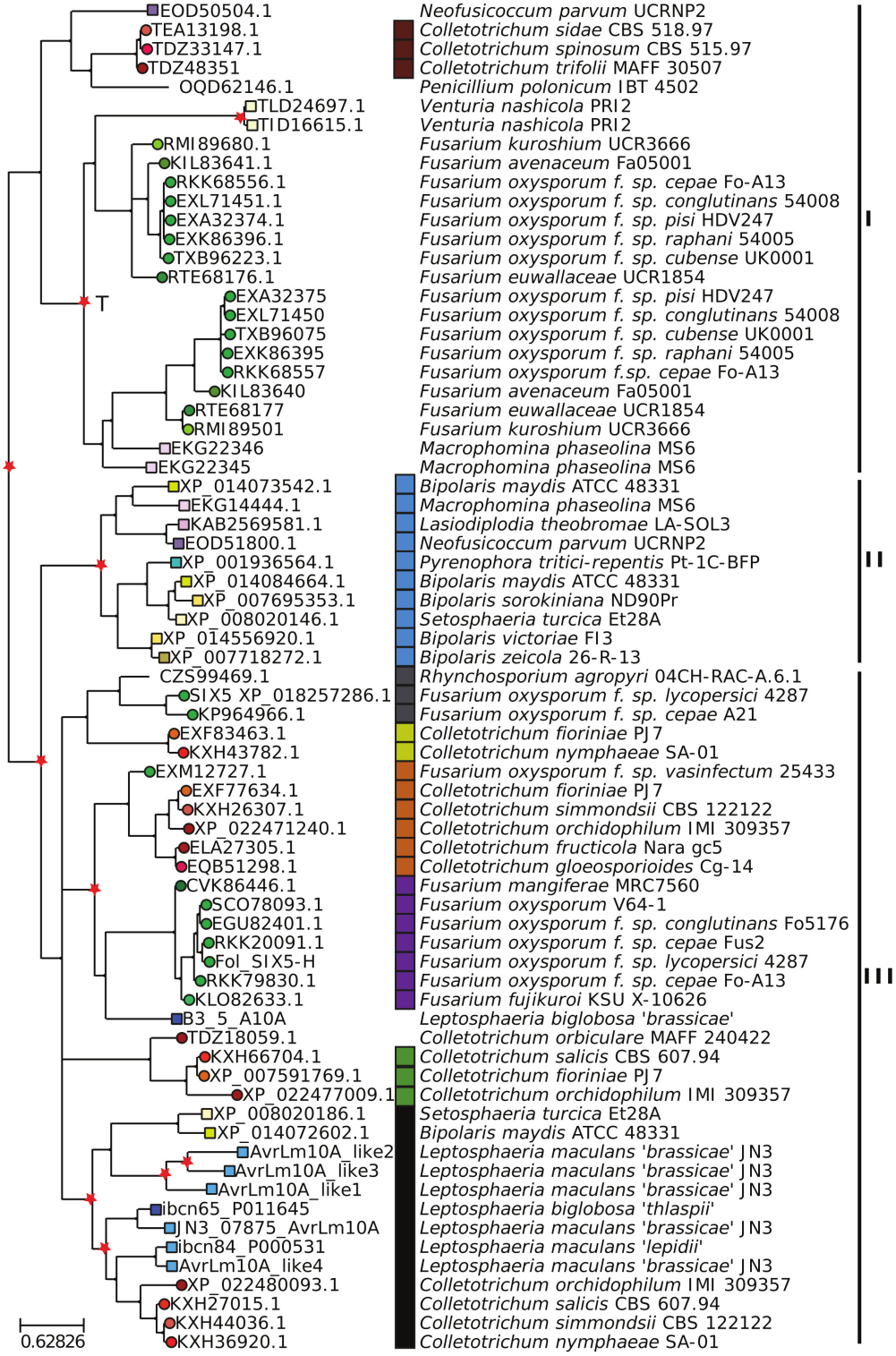

FIGURE 4 Eight different families of neighbouring genes cluster in the phylogenetic tree of AvrLm10A/SIX5 homologues. Maximum-likelihood phylogeny of AvrLm10A/SIX5 homologues listed in Table S5. The shape of terminal nodes indicates whether the protein is from a Sordariomycete (circle) or Dothideomycete (square) or other (no shape), nodes are coloured according to species and labelled with the protein identifier. Putative duplications are indicated with red stars. One tandem duplication is indicated with a "T": all *Fusarium* genes under that node are either adjacent to each other or at the end of separate contigs. The different families of neighbouring genes are indicated with coloured squares at the right side of the tree, together with species and strain names. The tree is divided into three main clades according to similarities in position of cysteines (Figure 5).

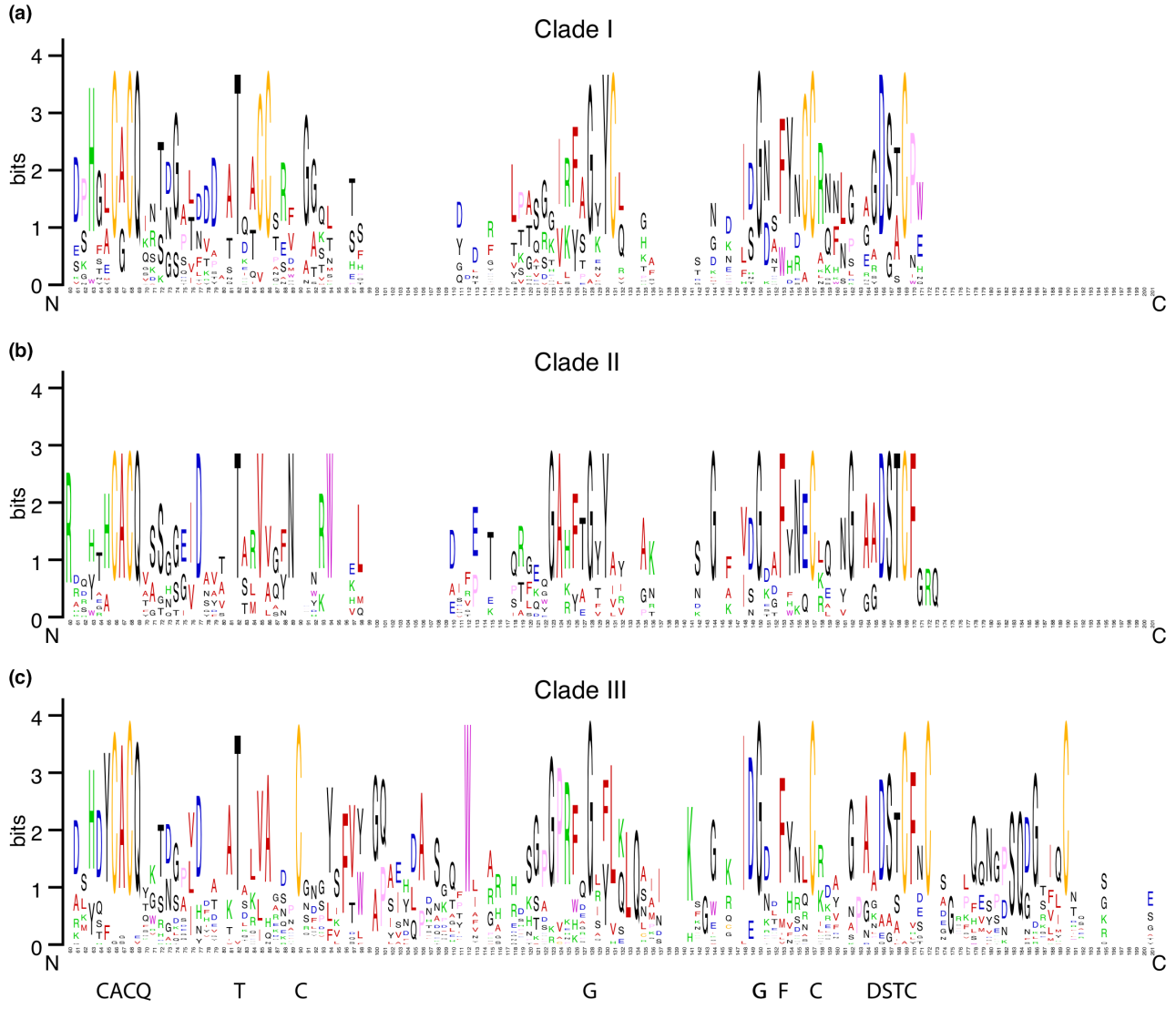

FIGURE 5 Sequence logos of three different subfamilies of AvrLm10A/SIX5 homologues. Sequence logos of amino acid sequences of the 25 proteins that belong to Clade I (a), of the 10 proteins that belong to Clade II (b), and of the 36 proteins that belong to Clade III (c) according to Figure 4. All sequence logos are based on position 60 to 201 in the multiple sequence alignment of AvrLm10A/SIX5 homologues and thus exclude the signal peptide. Conserved motifs in all clades are indicated at the bottom.

another protein that is not homologous to AvrLm10B, as already found for the effector pair SIX5/Avr2 (Cao et al., 2018; Ma et al., 2015). To identify putative nonorthologous replacements of AvrLm10B, we mined for neighbouring genes of AvrLm10A/SIX5 homologues in diverging transcriptional orientation and determined whether they encoded a small-secreted protein. Using that strategy, 36 neighbouring genes were found, separated by 633 to 7600 bp from AvrLm10A/SIX5 homologues. These proteins were variable in size, ranging from 111 to 295 amino acids, and cysteine number (between 0 and 12) and clustered into eight families, each of which is associated with a specific subfamily of AvrLm10A (Figure 4). When comparing concordance between the subfamilies of AvrLm10A and the phylogenies of the neighbouring genes, we find complete concordance in cases where the subfamily did not experience any duplications, and partial concordance otherwise (Figure S3). They are predicted as hypothetical proteins, with the exception of TEA13204, TDZ48352, and TDZ32965, which are predicted to encode acetylesterases (that annotation being questionable, as discussed in Petit-Houdenot et al., 2019). The conservation of local genome organization suggests functional interactions between AvrLm10A/SIX5 homologues and their neighbouring genes, even if these neighbours belong to different families.

3 | DISCUSSION

In this study, we characterized a family of effectors that are conserved in several fungal species, of which at least some have the peculiar capacity to form heterodimers with the protein encoded by a neighbouring gene in the opposite orientation. While fungal effectors have long been suggested to be species- or even subpopulation-specific, the availability of an increasing number of fungal genomic sequences, the prediction of fungal effector repertoires, and

resolution of their three-dimensional (3D) structure has enhanced the identification of homologous proteins and structural analogues among fungal effectors. Protein sequence similarities, while at a low level (typically less than 50% identity), have been detected for different effectors in plant-pathogenic fungi, illustrating possible conserved functions between species. This is, for instance, the case for the Avr4 effector that protects fungal hyphae against the hydrolytic activity of plant chitinases, and the LysM effector Ecp6 that prevents chitin-triggered plant immunity. These effectors were first described in *F. fulva* but are conserved in many Ascomycetes (De Jonge et al., 2010; Rocafort et al., 2020; Van Den Burg et al., 2006). Based on protein structure, several effector families were identified. This was the case for the RALPH (RNAse-Like Proteins Associated with Haustoria), MAX (for Magnaporthe Avrs and ToxB like), ToxA-like, and LARS (for Leptosphaeria AviRulence and Suppressing) effectors (De Guillen et al., 2015; Di et al., 2017; Lazar et al., 2022; Pedersen et al., 2012; Wang et al., 2007).

In this study, we characterized the AvrLm10 effector module of *L. maculans* that contains five pairs of homologues, including the AvrLm10A/AvrLm10B AVR proteins both necessary to trigger recognition by Rlm10 (Petit-Houdenot et al., 2019). We found that AvrLm10A homologues are widely conserved in Dothideomycete and Sordariomycete species but are associated with effectors belonging to a limited number of putative families. The conservation of AvrLm10A between unrelated plant-pathogenic fungi suggests that AvrLm10A and its homologues could have a similar function in distinct fungal species.

Seventy-one AvrLm10A homologues were found in 33 species of Dothideomycetes and Sordariomycetes, plus one in Eurotiomycete and one in Leotiomycete. Current phylogenomic analyses indicate shared ancestry between Sordariomycetes and Leotiomycetes, and possible shared ancestry between Dothideomycetes, Eurotiomycetes, and Lecanoromycetes (Li et al., 2021). That would mean neither Leotiomycetes nor Sordariomycetes are any closer to Dothideomycetes, and could mean the AvrLm10A/SIX5 homologues arose in an ancient shared Sordariomycetes/Dothideomycetes ancestor, with multiple subsequent losses in several classes.

The conservation of AvrLm10A/SIX5 in so many distinct species could be due to a function linked to their lifestyle during plant infection. With only two exceptions, all fungal species having maintained AvrLm10A/SIX5 homologues are phytopathogenic fungi classified as hemibiotrophs, that is, fungi having a relatively long biotrophic/asymptomatic life within plant tissues before inducing symptoms. These pathogens, along with pure biotrophs, are believed to use effectors to compromise plant defence responses during their asymptomatic life (Figueroa et al., 2021). The AvrLm10A/SIX5 family could therefore have an important role in the hemibiotrophic fungal lifestyle, possibly by favouring the biotrophic stage of infection before necrosis development. Indeed, suppression of *AvrLm10A* through silencing revealed a role of *AvrLm10A* in restricting leaf lesion development (Petit-Houdenot et al., 2019), thus lengthening the biotrophic stage of infection before the fungus switches to necrotrophy. Moreover, except for the *AvrLm10A_like4*/*AvrLm10B_like4* pair, all *AvrLm10* family gene pairs are specifically and highly expressed during asymptomatic stages of plant colonization, suggesting they play roles of biotrophic effectors during plant infection. In addition, the two distinct expression patterns observed suggest a potential relay between members of the AvrLm10 family during the long colonization of oilseed rape or distinct roles played during cotyledon and petiole/stem colonization.

The AvrLm10B member of the pair is also conserved in 10 species of Dothideomycetes and Sordariomycetes, but the remarkable feature of the AvrLm10A/SIX5 homologues is that they are organized as pairs of genes in inverse orientation with eight distinct families of effectors with no recognizable sequence identity between families, including AvrLm10B and Avr2. However, preliminary AlphaFold predictions suggest the 3D structure of AvrLm10B could show a β-sandwich fold similar to the Avr2 3D structure made up of two antiparallel sheets (Di et al., 2017). The proximity of the two genes within a pair and their tail-to-tail orientation could contribute to their simultaneous expression during infection. Indeed, it has been shown that SIX5 and Avr2 are under the control of a bidirectional promoter, implying a co-regulation and a simultaneous expression of these two genes (Ma et al., 2015). Moreover, the proximity of the two genes in the genome prevents the loss of one of them during chromosomal rearrangements, thus allowing their conservation in the populations.

The effector families associated with AvrLm10A homologues comprise between three and 15 members scattered between different species. Some are specific to the Sordariomycetes (such as the Avr2 family), while others such as the AvrLm10B family are found in Dothideomycetes and a few Sordariomycetes of the *Colletotrichum* genus. Within the genome of *Bipolaris maydis* and a few *Colletotrichum* species *AvrLm10A* homologues are paired with representatives of two distinct effector gene families. In contrast, in *L. maculans* 'brassicae', the five paralogues of *AvrLm10A* are all associated with a homologue of *AvrLm10B*. In *M. oryzae*, generation of paralogues of the avirulence gene *Avr-Pita* have been suggested to originate from a conserved copy in the essential genome (but deprived of avirulence activity) and duplicated multiple times via transpositions to other compartments of the genome such as subtelomeres (Chuma et al., 2011). From our data, it is tempting to speculate that the *AvrLm10A_like4/AvrLm10B_like4* pair, located in the essential genome but seemingly inactive, is the initial pair from which translocation/diversification in other genome compartments occurred.

The fact that we find the same or closely related species in different clades, and several AvrLm10A/SIX5 homologues in the same species, suggests that the AvrLm10A/SIX5 family experienced several rounds of duplication. However, horizontal transfer events, rather than duplication and independent losses, could also explain the patchy distribution we observe and the taxonomically "unlikely" grouping of evolutionary distant species. For example, the grouping of *Colletotrichum* species with *P. polonicum* in clade III and the grouping of *F. oxysporum* and *Colletotrichum* species with *R. agropyri* are probably best explained by introgressions or horizontal transfer. However, for most cases the extent of sequence divergence between the proteins in different subclades in the tree suggests a long period of diversification, consistent with ancestral duplications.

Members of the *AvrLm10* family are highly conserved in *L. maculans* field populations, except *AvrLm10A_like2/AvrLm10B_like2* that carry typical inactivation signatures (RIP mutations and deletions) and are present in only c.65% of isolates. In particular, both genes are absent in almost all the Mexican and more than 50% of the Australian isolates. This is typical of AVR genes that have been subjected to selection by a matching resistance gene (Rouxel & Balesdent, 2017). This suggests that *AvrLm10A_like2* and *AvrLm10B_like2* have been subjected to selection pressure by a still unknown resistance gene present in oilseed rape (and/or *Brassica oleracea*) grown in Australia and Mexico.

AvrLm10A and AvrLm10B can interact physically (Petit-Houdenot et al., 2019). Using two different approaches (FRET-FLIM and CoIP), we found a clear physical interaction between AvrLm10A_like2 and AvrLm10B_like2. Similarly, SIX5 functions in a pair with Avr2, the two effectors being also able to interact physically. Avr2 was found to contribute to virulence on susceptible tomatoes and recently demonstrated to target an evolutionarily conserved immune pathway (probably an early component of PAMP-triggered immunity signalling) acting as an adaptor protein to modulate cell-signalling cascades, SIX5 mediating movement of Avr2 from cell to cell via plasmodesmata (Cao et al., 2018; Di et al., 2017). This suggests that AvrLm10A and AvrLm10A_like2 may have the ability to transport their partner proteins from cell to cell during early infection of *L. maculans* leaves, but also possibly other effectors, as suggested by cross-interaction experiments (Table S4). By contrast, AvrLm10A_like1 could have lost that ability or, as the AvrLm10A_like1/AvrLm10B_like1 pair is produced specifically in petioles and stem, AvrLm10B_like1 may no longer be required to be transmitted from cell to cell via plasmodesmata. AvrLm10A_like1 could have acquired a distinct function in these tissues, as previously found for See1 from *Ustilago maydis*, which is required for the reactivation of plant DNA synthesis and affects tumour progression in leaf cells but does not affect tumour formation in immature tassel floral tissues (Redkar et al., 2015). This would indicate neofunctionalization and at least partly nonredundant functions of the four gene pairs.

In conclusion, the conservation of AvrLm10A/SIX5 suggests a general function for these effector proteins in cooperating with a limited number of other effectors. Moreover, the finding that most effectors belong to more or less conserved families suggests resistance genes targeting these families may exist or may be engineered to allow recognition of more than one pathogen, and thus may be used to develop broad-spectrum resistance to hemibiotrophic pathogens.

4 | EXPERIMENTAL PROCEDURES

4.1 | Fungal isolates and culture conditions

The isolates of *L. maculans* used in this study were collected from either naturally or experimentally infected plants (Table S2). The genome of the v23.1.3 strain was completely sequenced and annotated, and used as the reference *L. maculans* isolate (Dutreux et al., 2018; Rouxel et al., 2011). v23.1.2 is a sister strain of v23.1.3. All fungal cultures were maintained on V8 juice agar medium and conidiospores were collected as previously described by Ansan-Melayah et al. (1995).

4.2 | Bacterial strains and vector constructions

Genes of interest were amplified using specific primer pairs (Table S1) on cDNA of v23.1.3 using the *Taq* DNA polymerase Phusion (Invitrogen) under standard PCR conditions. Using a Gateway cloning strategy, PCR products flanked by attB recombination sites were recombined into the pDONR221 vector (Invitrogen) via a BP recombination reaction according to the supplier's recommendations (https://www.thermofisher.com/fr/fr/home/life-science/cloning/gateway-cloning/protocols.html#bp). *Escherichia coli* DH5α (Invitrogen) was used for the amplification of the Entry vectors. *E. coli* transformants were selected on Luria Bertani (LB) medium with 50 μg/mL of kanamycin. Inserts cloned into Entry vectors were subsequently inserted into different Destination vectors: pSite-Dest-RFP, pSite-Dest-GFP, pSite-RFP-Dest, and pSite-GFP-Dest via a LR recombination. *Agrobacterium tumefaciens* GV3101::pMP90 was then transformed with the Destination vectors.

4.3 | DNA extraction, PCR, and sequencing

Genomic DNA was extracted from *L. maculans* conidia with the DNeasy 96 plant kit (Qiagen) as described previously (Attard et al., 2002). *AvrLm10A*, *AvrLm10B*, and their homologues were amplified by PCR using primer pairs located in the 5′ and 3′ UTR of the genes (Table S1) using GoTaq G2 Flexi DNA polymerase (Promega) and a Mastercycler gradient thermocycler (Eppendorf). PCR products were sequenced by Eurofins Genomics. Sequences were aligned and compared using DNASTAR Lasergene software (v. 12.2.0.80).

4.4 | Identification of homologues and phylogenetic analyses

AvrLm10A/AvrLm10B homologues were identified in *L. maculans* 'brassicae' and closely related species by performing a BlastP analysis with BioEdit software (Hall, 1999) against the proteomes of *L. maculans* 'brassicae' (v23.1.3), *L. maculans* 'lepidii' (IBCN84), *L. biglobosa* 'thlaspii' (IBCN65), and *L. biglobosa* 'brassicae' (B3.5) available on https://bioinfo.bioger.inrae.fr/portal/data-browser/public/leptosphaeria/genomes.

BlastP analyses were then performed against the NCBI online databases using the five AvrLm10 protein pairs of *L. maculans* and SIX5 of *F. oxysporum* f. sp. *lycopersici* as queries. The criteria used to filter the homologues included e-value (<0.1), percentage of coverage (>65%), and sequence size (maximum size of 200 bp). We then aligned all protein homologues against a v23.1.3 proteome database using BioEdit to find the best reciprocal Blast. To complete the search for AvrLm10B homologues, an approach based on synteny was used. Both NCBI and Ensembl Fungi were used to identify the closest neighbouring genes

of *AvrLm10A/SIX5* homologues in opposite transcriptional orientation. Amino acid sequences of AvrLm10A homologues were aligned with m-coffee using the webserver (http://tcoffee.crg.cat/apps/tcoffee/do:mcoffee; Moretti et al., 2007). The multiple sequence alignment was adjusted manually to realign a few cysteines. Based on this curated multiple sequence alignment, we searched for the best substitution model with ModelFinder (WAG+R4) and inferred a maximum-likelihood phylogenetic tree with IQtree (2.1.4-beta) with 1000 bootstrapping replicates (Hoang et al., 2018; Kalyaanamoorthy et al., 2017; Minh et al., 2020). We collapsed all branches with bootstrap support below 60% and visualized the tree with ete3 (https://pypi.org/project/ete3/). The strategy to determine phylogenetic concordance is presented in Methods S1.

4.5 | RNA-seq analysis

Expression of the *AvrLm10* gene family was investigated using RNA-seq data generated by Gay et al. (2021) (see Methods S2). Reads from Darmor-*bzh* cotyledons, petioles, and stems inoculated with pycnidiospores of *L. maculans* isolate v23.1.2 were analysed as described by Gay et al. (2021). Reads from v23.1.2 grown on V8 agar were used as control. Two biological replicates were analysed per condition. For *AvrLm10A_like4* and *AvrLm10B_like4*, an alignment against RNA-seq reads under controlled conditions was again performed after manually correcting the two sequences.

4.6 | RT-qPCR analysis

RNA samples generated by Gay et al. (2021) were adjusted to 3 μg to generate cDNA using oligo-dT with the SMARTScribe reverse transcriptase (Clontech) according to the manufacturer's protocol. RNA samples corresponded to several infection stages of *L. maculans* v23.1.2 isolate on the susceptible cultivar of *B. napus* 'Darmor-*bzh*'. RT-qPCR experiments were performed using a 7900 real-time PCR system (Applied Biosystems) and ABsolute SYBR Green ROX dUTP Mix (ABgene) as described by Fudal et al. (2007). For each condition, two independent biological and two technical replicates were performed. The RT-qPCR primers used are indicated in Table S1. Cycles threshold (C_t) values were analysed as described by Muller et al. (2002) using the reference gene *EF1α*.

4.7 | Transient expression assays

A. tumefaciens GV3101::pMP90 expressing the different genes of interest fused to GFP or RFP were grown as described by Petit-Houdenot et al. (2019) and infiltrated in 4- to 5-week-old *N. benthamiana* leaves using a 1-mL syringe. The infiltrated plants were incubated for 48 h in growth chambers with 16 h of day (25°C, 50% humidity) and 8 h of night (22°C, 50% humidity) for FRET-FLIM, co-immunoprecipitation or colocalization experiments.

4.8 | Confocal laser scanning microscopy

Microscopy analyses were performed using a Leica TCS SPE laser scanning confocal microscope and a 63× oil objective lens. *N. benthamiana* leaves were observed 48 h postinfiltration. The following excitation and emission wavelengths were used: GFP, excitation 488 nm, emission captured using a 498–522/558 nm band-pass filter; RFP, excitation 532 nm, emission 556–621/656 nm. The detector gain was between 800 and 900, with an amplifier offset of −0.6. All images are representative of at least 20 scans.

4.9 | FRET-FLIM and data analysis

The fluorescence lifetime of the donor was measured in the presence and absence of the acceptor. FRET efficiency (*E*) was calculated by comparing the lifetime of the donor (AvrLm10A_like1-GFP or AvrLm10A_like2-GFP) in the presence (τDA) or absence (τD) of the acceptor (AvrLm10B_like1-RFP, AvrLm10B_like2-RFP, RFP-AvrLm10B_like1 or LmStee98-RFP): $E = 1 - (\tau DA)/(\tau D)$. Statistical comparisons between control (donor) and assay (donor + acceptor) lifetime values were performed by Student's *t* test. FRET-FLIM measurements were performed using a FLIM system coupled to a streak camera (Krishnan et al., 2003) as described in Petit-Houdenot et al. (2019). For each cell, average fluorescence decay profiles were plotted and lifetimes were estimated by fitting data with an exponential function using a nonlinear least-squares estimation procedure (detailed in Camborde et al., 2017).

4.10 | Protein extraction, western blot, and co-immunoprecipitation

AvrLm10A_like1-GFP/AvrLm10B_like1-RFP or AvrLm10A_like2-GFP/AvrLm10B_like2-RFP were co-expressed in *N. benthamiana* leaves. AvrLm10A_like1-GFP and AvrLm10A_like2-GFP were co-expressed with RFP as a negative control. Forty-eight hours after infiltration, proteins from 1 g of *N. benthamiana* leaves were extracted as described by Petit-Houdenot et al. (2019).

For immunodetection, extracted proteins were mixed with 4× Laemmli sample buffer (Bio-Rad) and boiled for 5 min. For immunoprecipitation, 20 mL of magnetic RFP-trap M beads (RFP-Trap Chromotek) were prewashed in the protein extraction buffer, added to the protein extract and gently agitated for 3 h at 4°C. The beads were washed four times with the protein extraction buffer, then once with low salt washing buffer (20 mM Tris HCl, pH 7.5). The proteins were eluted by boiling in 4× Laemmli sample buffer for 5 min.

Proteins were run on a 10% polyacrylamide gel containing SDS, blotted onto PVDF membranes using semidry blotting for 30 min at 15 V (Bio-Rad) and analysed by immunoblotting using monoclonal anti-RFP (RF5R) antibody (Thermo Fisher) or anti-GFP antibody (Invitrogen) and a secondary goat-anti-mouse antibody conjugated with horseradish peroxidase (Dako) as described by Petit-Houdenot et al. (2019).

ACKNOWLEDGEMENTS

Authors wish to thank all members of the Effectors and Pathogenesis of *L. maculans* group. We are grateful to the BIOGER bioinformatics platform (https://bioinfo.bioger.inrae.fr/; Nicolas Lapalu, Adeline Simon) for their helpful discussions. N.T. was funded by a PhD salary from the University Paris-Saclay and Y.P.-H. by a Contrat Jeune Scientifique grant from INRAE. The Effectors and Pathogenesis of *L. maculans* group benefits from the support of Saclay Plant Sciences-SPS (ANR-17-EUR-0007). This work was supported by the French National Research Agency project StructuraLEP (ANR-14-CE19-0019). The LIPME is part of the French Laboratory of Excellence project (TULIP ANR-10-LABX-41).

DATA AVAILABILITY STATEMENT

AvrLm10A/AvrLm10B homologues were identified in *L. maculans* 'brassicae' and closely related species by performing a BlastP analysis with BioEdit software (Hall, 1999) against the proteomes of *L. maculans* 'brassicae' (v23.1.3), *L. maculans* 'lepidii' (IBCN84), *L. biglobosa* 'thlaspii' (IBCN65), and *L. biglobosa* 'brassicae' (B3.5) available on https://bioinfo.bioger.inrae.fr/portal/data-browser/public/leptosphaeria/genomes.

ORCID

Like Fokkens https://orcid.org/0000-0001-6696-4409
Thierry Rouxel https://orcid.org/0000-0001-9563-1793
Marie-Hélène Balesdent https://orcid.org/0000-0001-5523-9180
Martijn Rep https://orcid.org/0000-0003-3608-6283
Isabelle Fudal https://orcid.org/0000-0002-9105-9432

REFERENCES

Ansan-Melayah, D., Balesdent, M.-H., Buee, M.M. & Rouxel, T.T. (1995) Genetic characterization of *AvrLm1*, the first avirulence gene of *Leptosphaeria maculans*. *Phytopathology*, 85, 1525–1529.

Attard, A., Gout, L., Gourgues, M., Kühn, M.-L., Schmit, J., Laroche, S. et al. (2002) Analysis of molecular markers genetically linked to the *Leptosphaeria maculans* avirulence gene *AvrLm1* in field populations indicates a highly conserved event leading to virulence on *Rlm1* genotypes. *Molecular Plant-Microbe Interactions*, 15, 672–682.

Ayukawa, Y., Asai, S., Gan, P., Tsushima, A., Ichihashi, Y., Shibata, A. et al. (2021) A pair of effectors encoded on a conditionally dispensable chromosome of *Fusarium oxysporum* suppress host-specific immunity. *Communications Biology*, 4, 707.

Balesdent, M.-H., Fudal, I., Ollivier, B., Bally, P., Grandaubert, J., Eber, F. et al. (2013) The dispensable chromosome of *Leptosphaeria maculans* shelters an effector gene conferring avirulence towards *Brassica rapa*. *New Phytologist*, 198, 887–898.

Brun, H., Chèvre, A.-M., Fitt, B.D.L., Powers, S., Besnard, A.-L., Ermel, M. et al. (2010) Quantitative resistance increases the durability of qualitative resistance to *Leptosphaeria maculans* in *Brassica napus*. *New Phytologist*, 185, 285–299.

Camborde, L., Jauneau, A., Brière, C., Deslandes, L., Dumas, B. & Gaulin, E. (2017) Detection of nucleic acid–protein interactions in plant leaves using fluorescence lifetime imaging microscopy. *Nature Protocols*, 12, 1933–1950.

Cao, L., Blekemolen, M.C., Tintor, N., Cornelissen, B.J.C. & Takken, F.L.W. (2018) The *Fusarium oxysporum* Avr2-Six5 effector pair alters plasmodesmatal exclusion selectivity to facilitate cell-to-cell movement of Avr2. *Molecular Plant*, 11, 691–705.

Chuma, I., Isobe, C., Hotta, Y., Ibaragi, K., Futamata, N., Kusaba, M. et al. (2011) Multiple translocation of the *AVR-Pita* effector gene among chromosomes of the rice blast fungus *Magnaporthe oryzae* and related species. *PLoS Pathogens*, 7, e1002147.

Daverdin, G., Rouxel, T., Gout, L., Aubertot, J.-N., Fudal, I., Meyer, M. et al. (2012) Genome structure and reproductive behaviour influence the evolutionary potential of a fungal phytopathogen. *PLoS Pathogens*, 8, e1003020.

De Guillen, K., Ortiz-Vallejo, D., Gracy, J., Fournier, E., Kroj, T. & Padilla, A. (2015) Structure analysis uncovers a highly diverse but structurally conserved effector family in phytopathogenic fungi. *PLoS Pathogens*, 11, e1005228.

De Jonge, R., Peter van Esse, H., Kombrink, A., Shinya, T., Desaki, Y., Bours, R. et al. (2010) Conserved fungal LysM effector Ecp6 prevents chitin-triggered immunity in plants. *Science*, 329, 953–955.

Degrave, A., Wagner, M., George, P., Coudard, L., Pinochet, X., Ermel, M. et al. (2021) A new avirulence gene of *Leptosphaeria maculans*, *AvrLm14*, identifies a resistance source in American broccoli (*Brassica oleracea*) genotypes. *Molecular Plant Pathology*, 22, 1599–1612.

Delourme, R., Pilet-Nayel, M.L., Archipiano, M., Horvais, R., Tanguy, X., Rouxel, T. et al. (2004) A cluster of major specific resistance genes to *Leptosphaeria maculans* in *Brassica napus*. *Phytopathology*, 94, 578–583.

Di, X., Cao, L., Hughes, R.K., Tintor, N., Banfield, M.J. & Takken, F.L.W. (2017) Structure-function analysis of the *Fusarium oxysporum* Avr2 effector allows uncoupling of its immune-suppressing activity from recognition. *New Phytologist*, 216, 897–914.

Dutreux, F., Da Silva, C., d'Agata, L., Couloux, A., Gay, E.J., Istace, B. et al. (2018) *De novo* assembly and annotation of three *Leptosphaeria* genomes using Oxford Nanopore MinION sequencing. *Scientific Data*, 5, 180235.

Figueroa, M., Ortiz, D. & Henningsen, E.C. (2021) Tactics of host manipulation by intracellular effectors from plant pathogenic fungi. *Current Opinion in Plant Biology*, 62, 102054.

Fudal, I., Ross, S., Brun, H., Besnard, A.-L., Ermel, M., Kuhn, M.-L. et al. (2009) Repeat-induced point mutation (RIP) as an alternative mechanism of evolution toward virulence in *Leptosphaeria maculans*. *Molecular Plant-Microbe Interactions*, 22, 932–941.

Fudal, I., Ross, S., Gout, L., Blaise, F., Kuhn, M.L., Eckert, M.R. et al. (2007) Heterochromatin-like regions as ecological niches for avirulence genes in the *Leptosphaeria maculans* genome: map-based cloning of *AvrLm6*. *Molecular Plant-Microbe Interactions*, 20, 459–470.

Galagan, J.E., Calvo, S.E., Borkovich, K.A., Selker, E.U., Read, N.D., Jaffe, D. et al. (2003) The genome sequence of the filamentous fungus *Neurospora crassa*. *Nature*, 422, 859–868.

Gay, E.J., Soyer, J.L., Lapalu, N., Linglin, J., Fudal, I., Da Silva, C. et al. (2021) Large-scale transcriptomics to dissect 2 years of the life of a fungal phytopathogen interacting with its host plant. *BMC Biology*, 19, 55.

Ghanbarnia, K., Fudal, I., Larkan, N.J., Links, M.G., Balesdent, M.-H., Profotova, B. et al. (2015) Rapid identification of the *Leptosphaeria maculans* avirulence gene *AvrLm2* using an intraspecific comparative genomics approach. *Molecular Plant Pathology*, 16, 699–709.

Ghanbarnia, K., Ma, L., Larkan, N.J., Haddadi, P., Fernando, W.G.D. & Borhan, M.H. (2018) *Leptosphaeria maculans* AvrLm9: a new player in the game of hide and seek with AvrLm4-7. *Molecular Plant Pathology*, 19, 1754–1764.

Gout, L., Fudal, I., Kuhn, M.-L., Blaise, F., Eckert, M., Cattolico, L. et al. (2006) Lost in the middle of nowhere: the *AvrLm1* avirulence gene of the dothideomycete *Leptosphaeria maculans*. *Molecular Microbiology*, 60, 67–80.

Grandaubert, J., Lowe, R.G., Soyer, J.L., Schoch, C.L., Van de Wouw, A.P., Fudal, I. et al. (2014) Transposable element-assisted evolution and adaptation to host plant within the *Leptosphaeria*

maculans-Leptosphaeria biglobosa species complex of fungal pathogens. *BMC Genomics*, 15, 891.
Guttman, D.S., McHardy, A.C. & Schulze-Lefert, P. (2014) Microbial genome-enabled insights into plant–microorganism interactions. *Nature Reviews Genetics*, 15, 797–813.
Hall, T.A. (1999) BioEdit: a user-friendly biological sequence alignment editor and analysis program for Windows 95/98/NT. *Nucleic Acids Symposium Server*, 41, 95–98.
Hoang, D.T., Chernomor, O., Von Haeseler, A., Minh, B.Q. & Vinh, L.S. (2018) UFBoot2: improving the ultrafast bootstrap approximation. *Molecular Biology and Evolution*, 35, 518–522.
Jiquel, A. (2021) *Exploitation du répertoire d'effecteurs de Leptosphaeria maculans pour une diversification des sources de résistance à la nécrose du collet chez Brassica napus*. PhD thesis. Paris: Université Paris-Saclay.
Jiquel, A., Gervais, J., Geistodt-Kiener, A., Delourme, R., Gay, E.J., Ollivier, B. et al. (2021) A gene-for-gene interaction involving a "late" effector contributes to quantitative resistance to the stem canker disease in *Brassica napus*. *New Phytologist*, 231, 1510–1524.
Jones, J.D.G. & Dangl, J.L. (2006) The plant immune system. *Nature*, 444, 323–329.
Kalyaanamoorthy, S., Minh, B.Q., Wong, T.K., Von Haeseler, A. & Jermiin, L.S. (2017) ModelFinder: fast model selection for accurate phylogenetic estimates. *Nature Methods*, 14, 587–589.
Krishnan, R.V., Masuda, A., Centonze, V.F.E. & Herman, B.A. (2003) Quantitative imaging of protein–protein interactions by multiphoton fluorescence lifetime imaging microscopy using a streak camera. *Journal of Biomedical Optics*, 8, 362–367.
Lazar, N., Mesarich, C.H., Petit-Houdenot, Y., Talbi, N., De La Sierra-Gallay, I.L., Zélie, E. et al. (2022) A new family of structurally conserved fungal effectors displays epistatic interactions with plant resistance proteins. *PLoS Pathogens*, 18, e1010664.
Li, Y., Steenwyk, J.L., Chang, Y., Wang, Y., James, T.Y., Stajich, J.E. et al. (2021) A genome-scale phylogeny of the kingdom Fungi. *Current Biology*, 31, 1653–1665.e5.
Lo Presti, L., Lanver, D., Schweizer, G., Tanaka, S., Liang, L., Tollot, M. et al. (2015) Fungal effectors and plant susceptibility. *Annual Review of Plant Biology*, 66, 513–545.
Ma, L., Houterman, P.M., Gawehns, F., Cao, L., Sillo, F., Richter, H. et al. (2015) The *AVR2–SIX5* gene pair is required to activate *I-2*-mediated immunity in tomato. *New Phytologist*, 208, 507–518.
Mesarich, C.H., Ökmen, B., Rovenich, H., Griffiths, S.A., Wang, C., Karimi Jashni, M. et al. (2018) Specific hypersensitive response-associated recognition of new apoplastic effectors from *Cladosporium fulvum* in wild tomato. *Molecular Plant-Microbe Interactions*, 31, 145–162.
Minh, B.Q., Schmidt, H.A., Chernomor, O., Schrempf, D., Woodhams, M.D., von Haeseler, A. et al. (2020) IQ-TREE 2: new models and efficient methods for phylogenetic inference in the genomic era. *Molecular Biology and Evolution*, 37, 1530–1534.
Moretti, S., Armougom, F., Wallace, I.M., Higgins, D.G., Jongeneel, C.V. & Notredame, C. (2007) The M-coffee web server: a meta-method for computing multiple sequence alignments by combining alternative alignment methods. *Nucleic Acids Research*, 35, W645–W648.
Muller, P.Y., Janovjak, H., MIserez, A.R. & Dobbie, Z. (2002) Processing of gene expression data generated by quantitative real-time RT PCR. *BioTechniques*, 33, 514.
Neik, T.X., Ghanbarnia, K., Ollivier, B., Scheben, A., Severn-Ellis, A., Larkan, N.J. et al. (2022) Two independent approaches converge to the cloning of a new *Leptosphaeria maculans* avirulence effector gene, *AvrLmS-Lep2*. *Molecular Plant Pathology*, 23, 733–748.
Parlange, F., Daverdin, G., Fudal, I., Kuhn, M.-L., Balesdent, M.-H., Blaise, F. et al. (2009) *Leptosphaeria maculans* avirulence gene *AvrLm4-7* confers a dual recognition specificity by the *Rlm4* and *Rlm7* resistance genes of oilseed rape, and circumvents Rlm4-mediated recognition through a single amino acid change. *Molecular Microbiology*, 71, 851–863.
Pedersen, C., Loren, V., van Themaat, E., McGuffin, L.J., Abbott, J.C., Burgis, T.A. et al. (2012) Structure and evolution of barley powdery mildew effector candidates. *BMC Genomics*, 13, 694.
Petit-Houdenot, Y., Degrave, A., Meyer, M., Blaise, F., Ollivier, B., Marais, C.-L. et al. (2019) A two genes-for-one gene interaction between *Leptosphaeria maculans* and *Brassica napus*. *New Phytologist*, 223, 397–411.
Plissonneau, C., Daverdin, G., Ollivier, B., Blaise, F., Degrave, A., Fudal, I. et al. (2016) A game of hide and seek between avirulence genes *AvrLm4-7* and *AvrLm3* in *Leptosphaeria maculans*. *New Phytologist*, 209, 1613–1624.
Redkar, A., Hoser, R., Schilling, L., Zechmann, B., Krzymowska, M., Walbot, V. et al. (2015) A secreted effector protein of *Ustilago maydis* guides maize leaf cells to form tumors. *The Plant Cell*, 27, 1332–1351.
Rocafort, M., Fudal, I. & Mesarich, C.H. (2020) Apoplastic effector proteins of plant-associated fungi and oomycetes. *Current Opinion in Plant Biology*, 56, 9–19.
Rouxel, T. & Balesdent, M. (2017) Life, death and rebirth of avirulence effectors in a fungal pathogen of *Brassica* crops, *Leptosphaeria maculans*. *New Phytologist*, 214, 526–532.
Rouxel, T., Grandaubert, J., Hane, J.K., Hoede, C., Van De Wouw, A.P., Couloux, A. et al. (2011) Effector diversification within compartments of the *Leptosphaeria maculans* genome affected by repeat-induced point mutations. *Nature Communications*, 2, 202.
Sánchez-Vallet, A., Fouché, S., Fudal, I., Hartmann, F.E., Soyer, J.L., Tellier, A. et al. (2018) The genome biology of effector gene evolution in filamentous plant pathogens. *Annual Review of Phytopathology*, 56, 21–40.
Shiller, J., Van de Wouw, A.P., Taranto, A.P., Bowen, J.K., Dubois, D., Robinson, A. et al. (2015) A large family of *AvrLm6-like* genes in the apple and pear scab pathogens, *Venturia inaequalis* and *Venturia pirina*. *Frontiers in Plant Science*, 6, 980.
Van de Wouw, A.P., Lowe, R.G.T., Elliott, C.E., Dubois, D.J. & Howlett, B.J. (2014) An avirulence gene, *AvrLmJ1*, from the blackleg fungus, *Leptosphaeria maculans*, confers avirulence to *Brassica juncea* cultivars. *Molecular Plant Pathology*, 15, 523–530.
Van Den Burg, H.A., Harrison, S.J., Joosten, M.H.A.J., Vervoort, J. & De Wit, P.J.G.M. (2006) *Cladosporium fulvum* Avr4 protects fungal cell walls against hydrolysis by plant chitinases accumulating during infection. *Molecular Plant-Microbe Interactions*, 19, 1420–1430.
Wang, C.-I.A., Gunčar, G., Forwood, J.K., Teh, T., Catanzariti, A.-M., Lawrence, G.J. et al. (2007) Crystal structures of flax rust avirulence proteins AvrL567-A and -D reveal details of the structural basis for flax disease resistance specificity. *The Plant Cell*, 19, 2898–2912.

SUPPORTING INFORMATION

Additional supporting information can be found online in the Supporting Information section at the end of this article.

How to cite this article: Talbi, N., Fokkens, L., Audran, C., Petit-Houdenot, Y., Pouzet, C., Blaise, F. et al. (2023) The neighbouring genes *AvrLm10A* and *AvrLm10B* are part of a large multigene family of cooperating effector genes conserved in Dothideomycetes and Sordariomycetes. *Molecular Plant Pathology*, 24, 914–931. Available from: https://doi.org/10.1111/mpp.13338